Supporting Information

Effect of pH on the catalytic degradation of Rhodamine B by the synthesized CDs/g-C_3N_4/Cu_xO composites

Yulian Guo, Chunsun Zhou, Lijuan Fang, Zhongda Liu, Wen Li, Miao Yang*

School of Chemistry, Chemical Engineering and Life Sciences, Wuhan University of Technology, Wuhan 430070, China

Corresponding Author: M. Yang, yangmiao@whut.edu.cn

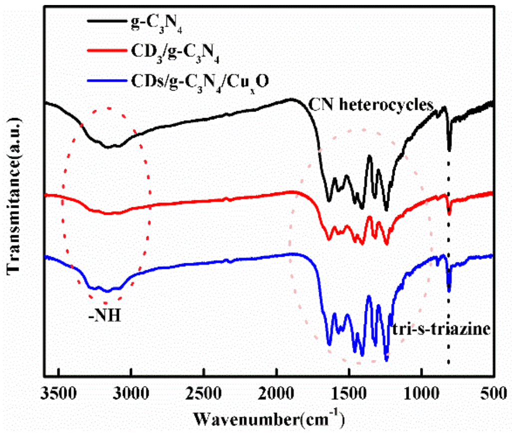

Figure S1. FT-IR spectra of g-C_3N_4, CD_3/g-C_3N_4, and CDs/g-C_3N_4/Cu_xO composite.

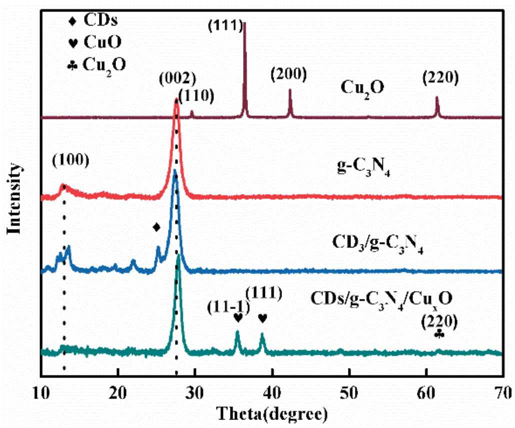

Figure S2. XRD patterns of Cu_2O, g-C_3N_4, CD_3/g-C_3N_4 and CDs/g-C_3N_4/Cu_xO composite.

Table S1. XPS results of the CDs/g-C_3N_4/Cu_xO composite.

	Binding energy/eV	Chemical bonds		Binding energy/eV	Chemical bonds
C 1s	284.94	C=C	N 1s	398.53	C−N=C
	287.90	C−OH		399.05	N−C_3
	288.31	N−C=N		400.73	C−N−H
Cu 2p	933.10/952.95	Cu^+ or Cu^0	Cu LMM	570.89	Cu^+
	935.02/955.13	Cu^{2+}		576.42	Cu^{2+}
	943.09/963.11	Cu^{2+} satellite peaks			

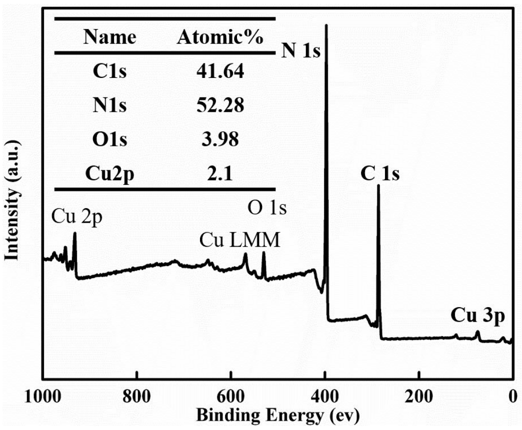

Figure S3. XPS spectra of CDs/g-C_3N_4/Cu_xO composite

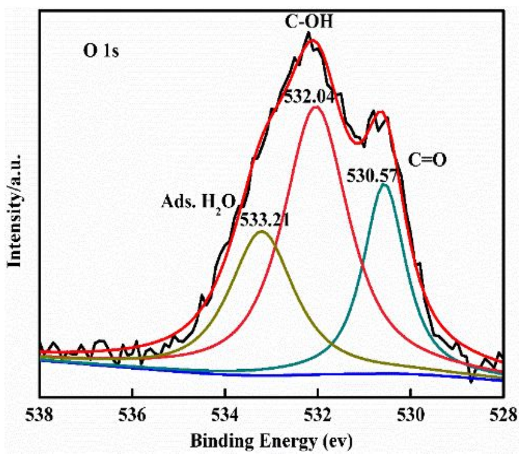

Figure S4. High-resolution XPS spectra of O1s

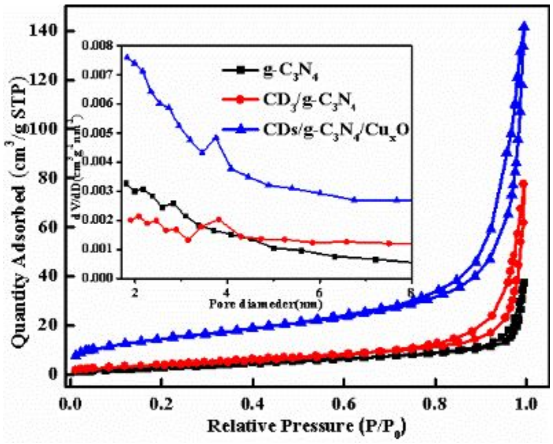

Figure S5. N_2 adsorption/desorption isotherm and the pore size distribution of g-C_3N_4, CD_3/g-C_3N_4, CDs/g-C_3N_4/Cu_xO.

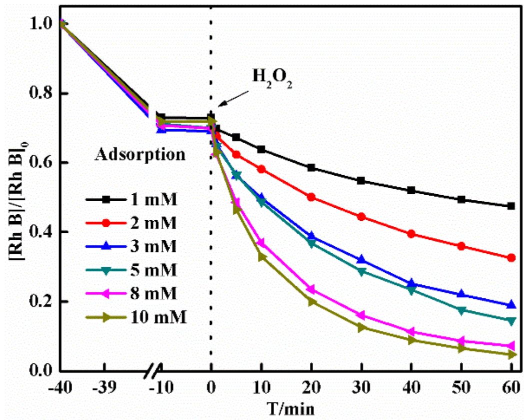

Figure S6. [Rh B]/[Rh B]$_0$ as a function of time with the different H_2O_2 concentrations in the presence of 2 g/L CDs/g-C_3N_4/Cu_xO composite with initial concentration of [Rh B]$_0$=0.064 mM, and V=100 mL.

Table S2. Utilization of H_2O_2 in the different H_2O_2 concentrations

$[H_2O_2]_0$(mM)	1	2	3	5	8	10
Degradation ratios (%)	52.6	67.4	81.1	85.4	92.8	95.2
Utilization (%)	4.1	3.1	2.1	3.3	2.1	2.5

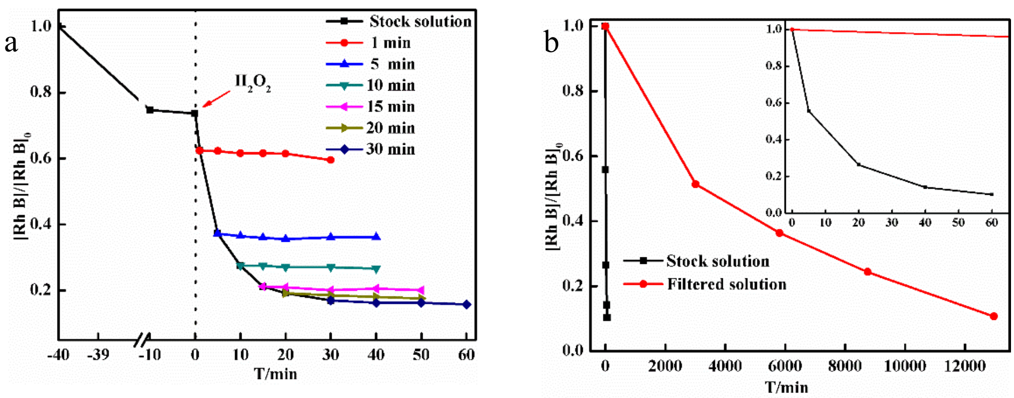

Figure S7. (a) [Rh B]/[Rh B]$_0$ as a function of time in stock CDs/g-C_3N_4/Cu_xO (2 g/L) suspensions and filtrates obtained at selected time intervals with initial concentration of [Rh B]$_0$=0.064 mM, [H_2O_2]$_0$=5 mM and V=100 mL. (b) Degradation of RhB in heterogeneous catalytic reaction and filtered solution in 1 min reacting over a longer period of time.

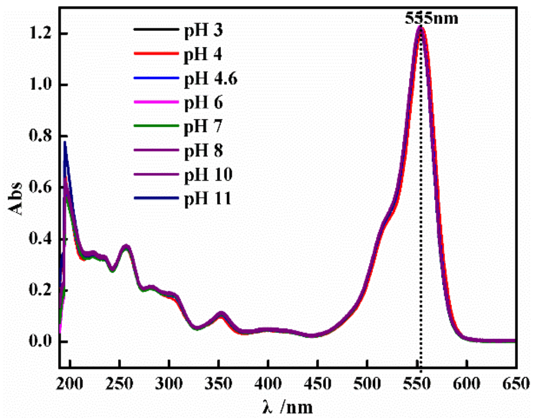

Figure S8. Variation of Rh B wavelength at different pH;

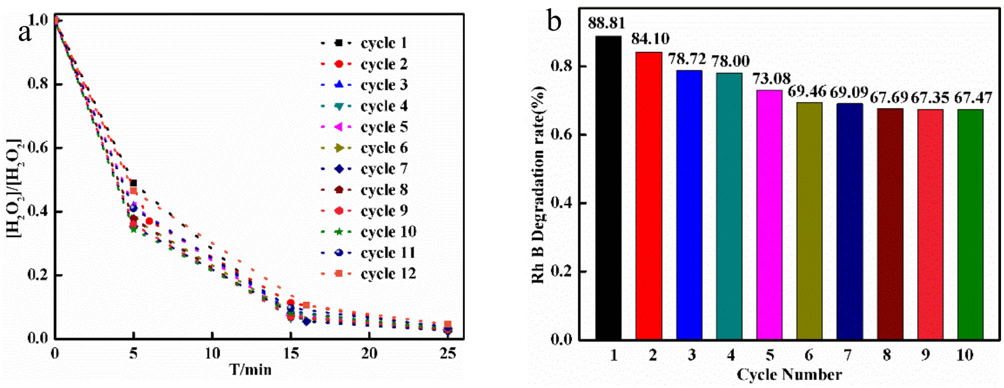

Figure S9. (a) Recycling performance for 5 mM H_2O_2 decomposition in the presence of 2 g/L CDs/g-C_3N_4/Cu_xO composite at pH 11 in 25 minutes per cycle, and V=100 mL; (b) Recycling performance of the 2 g/L CDs/g-C_3N_4/Cu_xO composite for Rh B (0.064 mM) degradation in the presence of 5 mM H_2O_2 at pH 11 in 30 minutes per cycle.

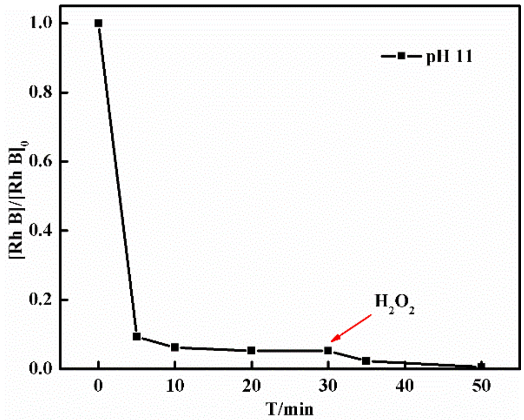

Figure S10. [Rh B]/[Rh B]$_0$ as a function of time in the presence of the 2 g/L CDs/g-C_3N_4/Cu_xO composite for Rh B (0.064 mM) degradation in the presence of 10 mM H_2O_2 at pH 11.

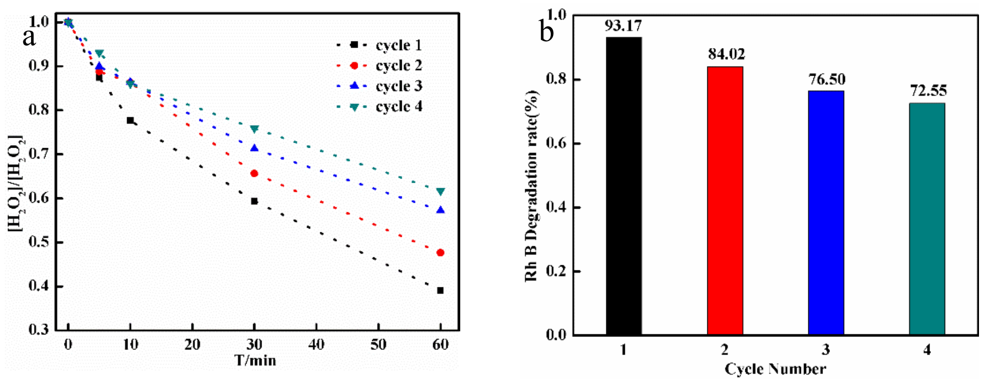

Figure S11. (a) H_2O_2 consumed in cycling reactions by the 2 g/L CDs/g-C_3N_4/Cu_xO composite for Rh B (0.064 mM) degradation in the presence of 5 mM H_2O_2 at pH 4.6 (Unadjusted pH; V=100 mL); (b) The recycling degradation of the Rh B (0.064 mM) was conducted by 2 g/L CDs/g-C_3N_4/Cu_xO composite in the presence of 5 mM H_2O_2 at pH 4.6 (unadjusted pH; V=100 mL).

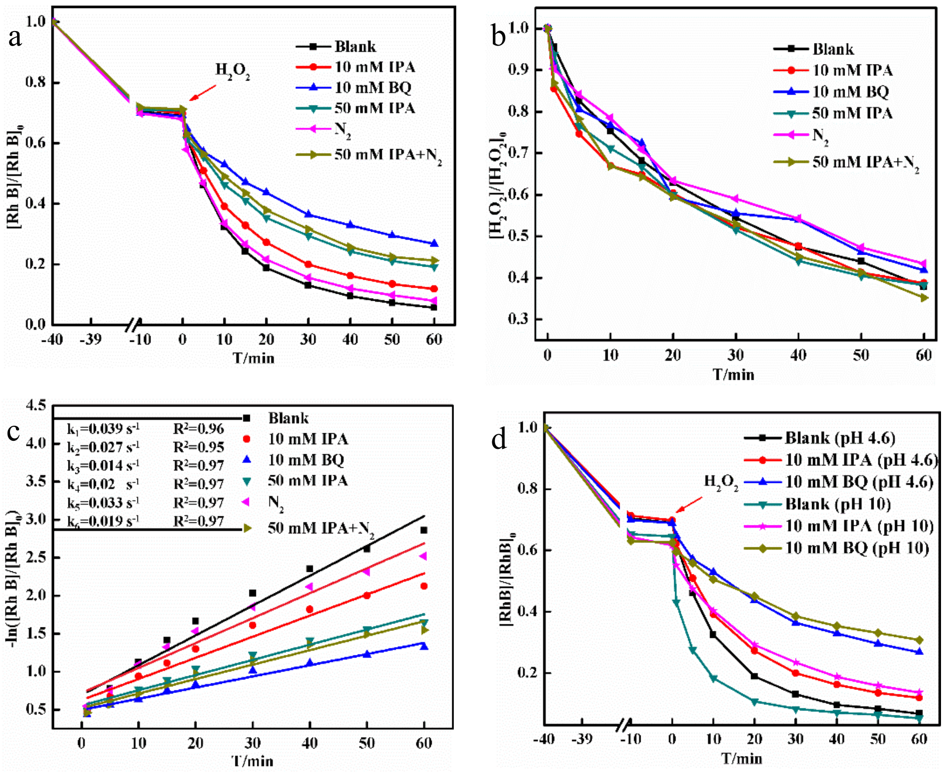

Figure S12. [Rh B]/[Rh B]$_0$ (a) and [H_2O_2]/[H_2O_2]$_0$ (b) as a function of time in the presence of different quenchers by the 2 g/L CDs/g-C_3N_4/Cu_xO composite for Rh B (0.064 mM) degradation in the presence of 5 mM H_2O_2. (c) Parameters of the pseudo-first-order kinetic models of different quenchers by the 2 g/L CDs/g-C_3N_4/Cu_xO composite for Rh B (0.064 mM) degradation in the presence of 5 mM H_2O_2. (d) [Rh B]/[Rh B]$_0$ as a function of time in the presence of different quenchers by the 2 g/L CDs/g-C_3N_4/Cu_xO composite for Rh B (0.064 mM) degradation in the presence of 5 mM H_2O_2 in different pH.

Table S3. Comparison of the catalytic performance of CDs/g-C_3N_4/Cu_xO and several reported relative studies.

Fenton-like Catalysts	Catalysts mg/mL	Pollutants	Cyclic degradation	The application range of pH	Ref.
CuNiFeLa-LDH	0.25	Antibiotics 10 mg/L	4 times 96.8%-96.5%	natural pH	58
Cu-MP NCs	1	Rh B 10 mg/L	6 times 99%-90%	2.62-10.42	59
Mn_3O_4.CuO	1.9	p-nitrophenol 10 mg/L	5 times 98%-78%	6-10	60
Cu/MnO_2	0.5	benzotriazole 5.96 mg/L	5 times 90%-39%	3.4-10.57	61
CDs/g-C_3N_4/Cu_xO	2.0	RhB 30 mg/L	8 times 99%-95%	3-11	This work

Table S4. Reaction formulas and reaction rate constants of possible reactions in radical trapping. [51, 53, 62]

Reaction formula	Reaction rate constant	Mark
•OH+BQ → BQ-•OH	$k = 6.6 \times 10^9\ M^{-1}\ s^{-1}$	R_1
$•O_2^-$+BQ→BQ-$•O_2^-$	$k = 0.9\text{-}1.0 \times 10^9\ M^{-1}\ s^{-1}$	R_2
•OH+ IPA→IPA-•OH	$k = 1.9 \times 10^9$ M−1 s−1	R_3
•OH + •OH → H_2O_2	$k = 5\text{-}8 \times 10^9\ M^{-1}\ s^{-1}$	R_4
•OH + H_2O_2 → $•O_2H$	$k = 1.7\text{-}4.5 \times 10^7\ M^{-1}\ s^{-1}$	R_5
$•O_2H$ + $•O_2H$ → $H_2O_2 + O_2$	$k = 0.8\text{-}2.2 \times 10^6\ M^{-1}\ s^{-1}$	R_6
•OH + $•O_2H$ → $H_2O + O_2$	$k = 1.4 \times 10^{10}\ M^{-1}\ s^{-1}$	R_7

Table S5. The initial mass ratio of Cu_2O to CDs/g-C_3N_4 for CDs/g-C_3N_4/Cu_xO composites.

S.NO	Sample code	wt% of Cu_2O
0.5	C1	1.3
1	C2	2.8
2	C3	5.4
3	C4	7.9
4	C5	10.0
5	C6	12.5